

RESEARCH AND DEVELOPMENT STATUS OF LOW POWER PULSED PLASMA THRUSTER SYSTEM FOR μ -Lab Sat II^{*†}

Naoki KUMAGAI[‡], Kensuke SATO[§], Kohji TAMURA[‡], Kentaro KAWAHARA[§]

Takahiro KOIDE[§], and Haruki TAKEGAHARA[¶]

Tokyo Metropolitan Institute of Technology, Dept. of Aerospace Eng.
Asahigaoka 6-6, Hino, Tokyo 191-0065, JAPAN
+81-42-585-8659,
ppt@astak3.tmit.ac.jp

Mitsuteru SUGIKI^{**}

Astro Research Corporation
Kugenuma Tachibana 1-1-4, Fujisawa, Kanagawa, 251-0024, JAPAN

Takashi WAKIZONO^{##}

HI-SERVE Corporation
Totohara 780-7, Akiruno, Tokyo, 190-0152, JAPAN

Hidekazu HASHIMOTO^{††}

National Space Development Agency of Japan
Advanced Mission Research Center, Micro Space Systems Laboratory
Sengen, 2-1-1, Tsukuba, Ibaraki 305-0047, JAPAN

IEPC-03-0202

Abstract

In this paper, the current of the design consideration and the present status of the research and development of TMIT-PPT for μ -Lab Sat II are described. In the design consideration of Thruster Head, in order to achieve the non charring and uniform sublimation area and the durability of long time operation, the change of the sublimation area (from 5.0 cm² to 0.5 cm²), discharge energy density (from 0.5 J/cm² to 7.2 J/cm²) and electrode material (from brass to molybdenum) were described. And in order to fix the design of EM assembly, the hood angle, capacitor, PPU configuration, system configuration and so on were fixed. At present, we have evaluated the validation of EM system. The impulse bit and specific impulse of EM Thruster Head are about 21.5 μ N-s and 960 s and the mass of EM PPT assembly is about 1.4 kg.

Introduction

In recent years, the demands for small satellites increase in order to realize the flexible and challenging

* Presented as Paper IEPC-03-? at the 28th International Electric Propulsion Conference, Toulouse, France, 17-21 March 2003.

† Copyright © 2003 by H. Takegahara, Published by Electric Rocket Propulsion Society with permission.

‡ Graduate Student, Student Member AIAA.

§ Graduate Student.

¶ Professor, Senior Member AIAA.

** President, Senior Member AIAA.

President

†† Senior Engineer.

mission which is independent on the large satellites, therefore the need for miniaturizing the thruster systems has become apparent. Pulsed plasma thruster (PPT) is one of the promising propulsion system for the small, micro- and nano-satellite attitude control, station keeping, de-orbit, formation flying, and drag compensation because of the following reasons.

1) Solid propellant advantages:

Propellant storage and management system such as reservoir tank, pressure transducer, valves and piping system, are not necessary.

2) Light weight and high reliability

It has only two power supplies for the thrust generation.

: Capacitor charge power supply and ignition power supply.

It has only one moving mechanism.

: Solid propellant feed mechanism into discharge chamber.

3) Small impulse bit level:

Precise total impulse control is possible.

These benefits make the PPT an attractive and reliable on-board propulsion alternative for orbit insertion, orbit maintenance, orbit raising and de-orbiting of small satellites. And also, it offers a small, discrete impulse bit which gives satellites mission advantages such as accurate positioning, attitude control, drag makeup, and constellation stationkeeping.

In Japan, PPT is a space-qualified devices and we have an experience that PPT had installed and operated successfully on ETS (Engineering Test Satellite)-IV launched in 1982.^{1,2} Considering the aforementioned requirements for small satellites, TMIT (Tokyo Metropolitan Institute of Technology) has started its R&D with the collaboration of NASDA for the application to the NASDA's μ -Lab Sat II.

μ -Lab Sat II³, shown in Fig. 1, is a 50kg-class piggyback satellite, and its main design concepts are as follows:

- Verification of 50kg class 3-axis Stabilized micro-Satellite Bus Technology
- Cable-saving using LAN System
- Low Bus Voltage ($3.6 \times n$ V)
- Short Development Period and Low Cost
- Puled Plasma Thruster Experiment on Orbit

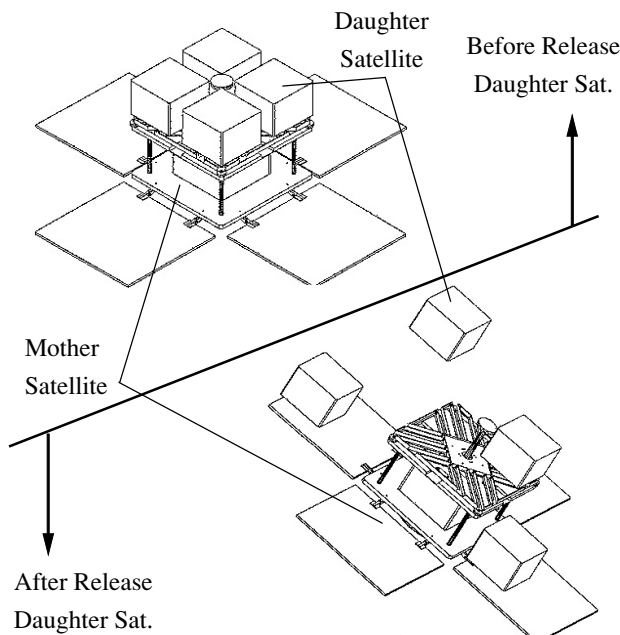


Fig. 1 μ -LabSat II³.

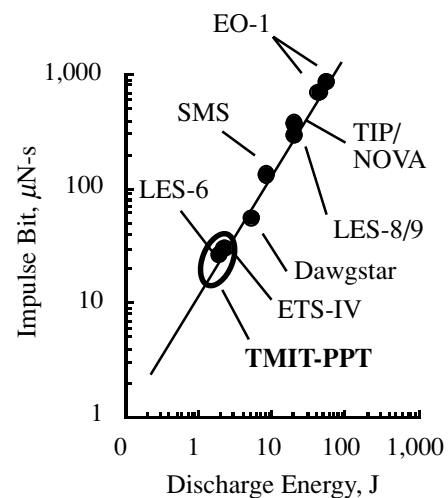


Fig. 2 Target of TMIT-PPT and flowing PPTs.^{2,4-7}

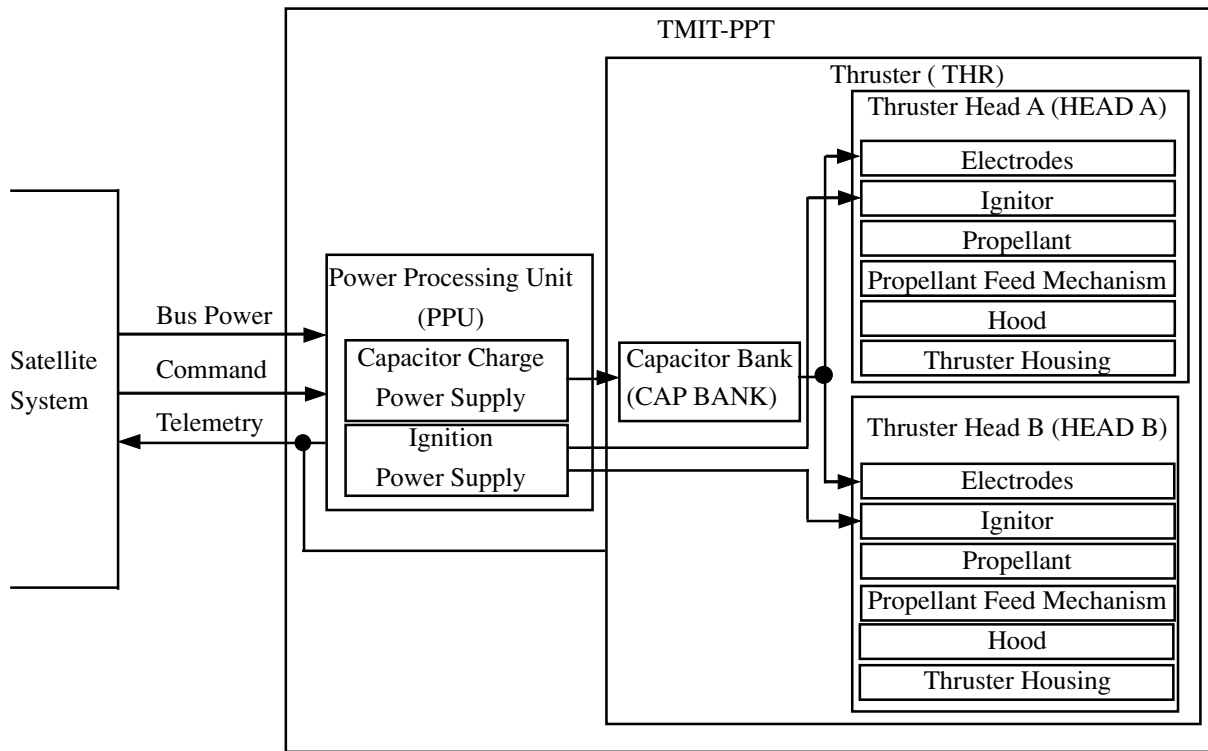


Fig. 3 TMIT PPT Subsystem Block Diagram.

System Design

Figure 2 shows the thrust level target of TMIT-PPT. Because μ -Lab Sat II requires the lightweight and low power consumption propulsion system, we try to achieve the lowest thrust level and power consumption PPT in the world. The block diagram of TMIT PPT subsystem is shown in Fig. 3. As shown in this figure, one TMIT PPT unit is composed of three components which are one PPU (including one capacitor charge power supply and one ignition power supply), one capacitor bank, and two thruster heads A/B (including electrodes, ignitor, propellant, propellant feed mechanism, thruster housing and hood respectively). As both electrodes of thruster head A and B are connected to the same capacitor bank, they have the same electrical potential at the same time as the capacitor bank is charged. The operation of thruster head is selected by the ignition command that delivers the high voltage ignition discharge to the cathode. And each of the three components is capable of separating and the relative position is variable freely for the feasibility of thruster system assembly.

Configuration Change of Thruster Head

The research and development of TMIT-PPT were based on ETS-IV PPE (Pulsed Plasma Engine) which was launched in 1982 and operated in space environment successfully. In this section, the currents of the design consideration of thruster head from ETS-IV PPE model to TMIT-PPT EM thruster head are described.

Attempts at Non Charring Sublimation Surface

When we started the study on TMIT-PPT, the successive firing test was conducted with ETS-IV EM (Engineering Model) thruster head and capacitor bank at 2.3 J. The electrode configuration of this thruster has a 25

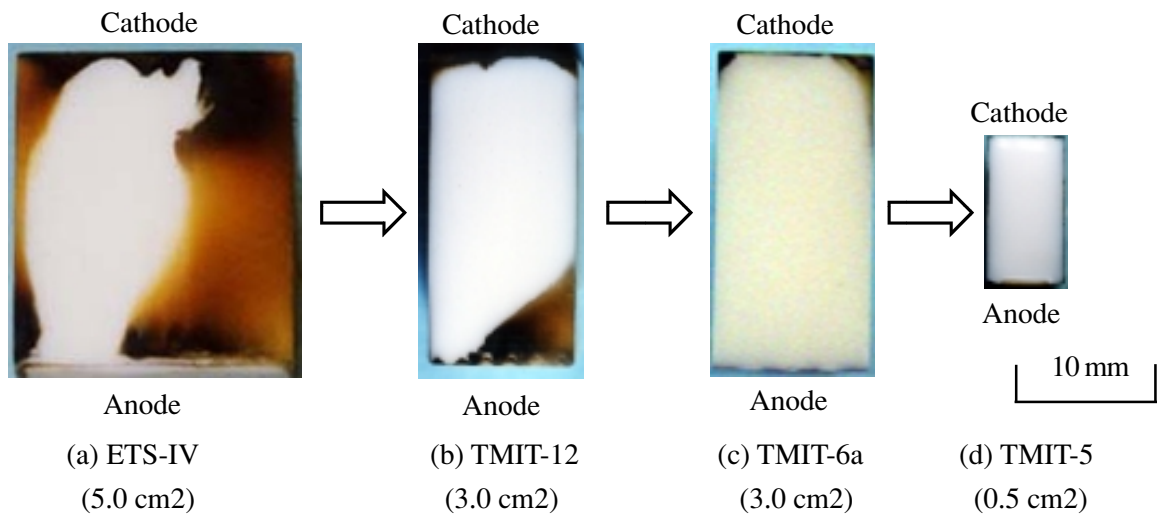


Fig. 4 Sublimation Condition of Each PPTs at 2.3 J

mm gap, with 20 mm wide by 40 mm long parallel electrode and the capacitance of capacitor bank is about 2.0 μF . But, from the beginning of this test, the charring was occurred on the sublimation surface. Because this charring problem was not improved as shown in Fig. 4(a), this test was stopped after 110,000 shots. After this successive test, though we conducted 10,000 shots operation of ETS-IV PPE for several times, the charring problem was not improved. Observing the sublimation surface, the edge of propellant surface was not ablated in the contrast with the center of it. So, we designed the TMIT-12 thruster whose electrode and propellant width were changed from 20 mm to 12 mm for the purpose of eliminating the charring area. The sublimation area of TMIT-12 operation at 2.3 J was shown in Fig. 4(b). As shown in this figure, compared with ETS-IV PPE, though the charring area was decreased, there was small charring area near TMIT-12 anode. Next, we designed the TMIT-6a thruster whose anode width were changed from 12 mm to 6 mm remaining the cathode width to be 12 mm compared with TMIT-12. But, the size of sublimation area of TMIT-6a propellant was remained to be same as the one of TMIT-12 (ie.12 mm wide \times 25 mm gap). By using TMIT-6a we could achieve non charring sublimation surface shown in Fig. 4(c), when the thruster was operated at 2.3 J.

Following the attainment of non charring sublimation surface, we evaluated the performance trends of TMIT-6a by changing the discharge energy between 2J and 35J. Figure 5 shows the trends of specific impulse with TMIT-6a against the energy density (this means discharge energy / sublimation area) at several energy com-

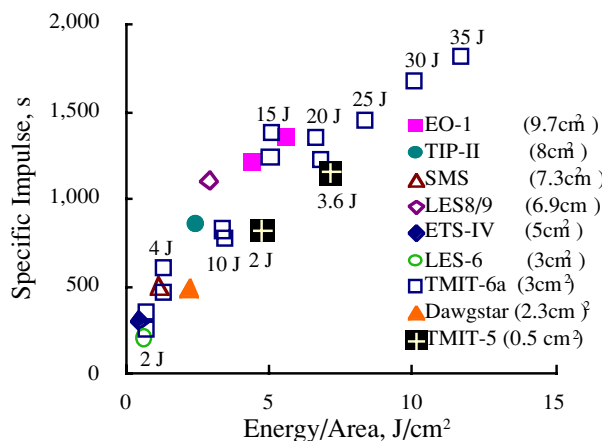


Fig. 5 Effect of Energy Density on Performance^{2,4,7}.

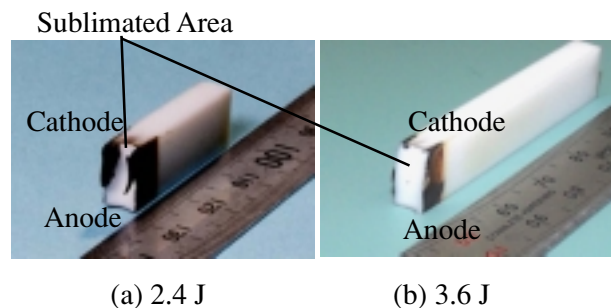


Fig. 6 Sublimation Condition after 100,000 shots.

Table 1 Characteristics of Brass and Molybdenum

	Brass	Mo
Melting Point, K	1,173	2,883
Thermal Conductivity, W/mK	106	139
Specific Heat, J/gK	0.377	0.3
Electrical Resistivity, Ωm	6×10^{-8}	5.6×10^{-8}

Table 2 Result of Change of Discharge Energy and Electrode Material

	Mo	Brass	Brass
Energy, J	3.6	3.6	2.4
Specific Impulse, sec	1129	1015	927
Impulse Bit, $\mu\text{ N-s}$	29.4	28	16.5
Mass Shot (Prop.), $\mu\text{ g}$	2.66	2.44	1.78
Cathode Erosion, $\mu\text{ g}$	0.114	0.252	0.115
Anode Erosion, $\mu\text{ g}$	0.041	0.195	0.112
Propellant Feed	OK	OK	NG

pared with the other PPTs in the world. As shown in this figure, it is obvious that the specific impulse of PPT depends on the energy density

Though we can improve the specific impulse by increasing the energy density, the improvement of specific impulse by increasing the discharge energy is not available in consideration for the PPT integration to small satellites. Therefore we designed TMIT-5 thruster head. TMIT-5 has a 10mm gap, with 5mm wide by 20mm long parallel electrode and more energy density by miniaturizing the propellant size than TMIT-6a. The sublimation area of TMIT-5 are shown in Fig. 4(d), and this area is much smaller than ETS-IV, TMIT-12 and TMIT-6a. Then, as shown in Fig. 5, the specific impulse of TMIT-5 corresponded with the performance trends of PPT predictably, and this scaling law of specific impulse of PPT seems to be useful for the design of PPT. At present, though the EM thruster heads have been evaluated, the design of EM thruster heads are almost the same as TMIT-5.

Change of Discharge Energy and Electrode Material

To feed the propellant smoothly and to reduce the electrode erosion, the effect of the change of discharge energy and electrode material were evaluated with the TMIT-5 type thruster heads. In case of 2.4 J operation, though the whole propellant surface was successfully ablated in the first 10,000 shots, no uniform ablation was occurred after 100,000 shots firing. As a result, because the charring was occurred at the edge of the sublimation area through the 100,000 shots firing shown in Fig. 6(a), the propellant was not fed to the specified position. In order to solve the non uniform ablation problem, we increased the discharge energy from 2.4 J to 3.6 J. Then, as shown in Fig. 6(b), the charring was not occurred at the edge of the sublimation area after 100,000 shots firing, and the propellant feed was successfully achieved.

As the result of increasing the discharge energy, however, the brass electrode was eroded severely and the ability of long time operation of brass electrode became uncertain. Then molybdenum electrode was evaluated instead of the brass electrode. The physical properties of the brass and molybdenum are shown in Table 1. As shown in this table, the properties which appear to have influence upon the PPT performance are almost same between brass and molybdenum except for the melting point. The difference between molybdenum and brass electrode at 3.6 J operation are shown in Table. 2, together with the result of 2.4 J operation with the brass electrode. As shown in this table, mass shot, impulse bit and specific impulse were greatly not different between brass and molybdenum electrode at 3.6 J, and the quantity of the cathode and anode erosion decreased to the half and one-fifth level.

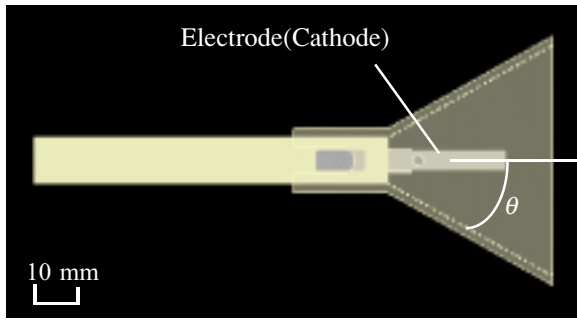


Fig.7 TMIT-PPT with θ degree hood.

Effect of Opening Angle of Hood on Performance

Considering the PPT integration to the satellite, the contamination shield hood is necessary to prevent the PPT plume from spreading and contaminating on the satellite surface. But, the opening angle of hood affect the PPT performance. For example, in the experiments of ETS-IV PPE, Hirata and Murakami⁸ reported that contamination distribution did not change with over about 40 degree hood and that narrower the opening angle of the hood became less than about 40 degree, narrower the contamination distribution was. Furthermore, in case of too narrow opening angle, the reduction of impulse bit was reported. Then, we have evaluated the effect of hood angle on the PPT performance with 0, 15, 30, 45, 60 degree hoods. In this experiment the hood angle θ is defined to be the half angle of the opening angle of hood as shown in Fig. 7. And in this experiment two type thruster heads were used. One was the TMIT-5 type with molybdenum electrodes, and the other was the TMIT-5 type with brass electrodes.

Figure 8 show the mass shot, impulse bit, and specific impulse of the operation with 0, 15, 30, 45, 60 degree hoods and without hood. In these figures, 180 degree points indicate the value of without hood operation. As shown in Fig. 8(a) and (b), the mass shot was greatly not different with each angle hoods and without hood. On the other hand, as shown in Fig. 8(b), the impulse bit with each of hoods indicated low values compared with the without hood operation, 0 degree operation particularly did in contrast with that 15, 30, 45, 60 degree hood operation provided almost the same impulse bit. Consequently, specific impulse with 0 degree hood indicated the lowest value, and specific impulse with 15, 30, 45, and 60 degree hood did the close value.

As the reason of impulse bit decrease with 0 degree hood, we can assume the momentum loss of plume by collision with the hood inner wall. In the other study on PPT plume, it was reported that the spread angle of charged particles ejected from PPT is about 30 - 40 degree⁹⁻¹¹. If the spread angle of charged particles is

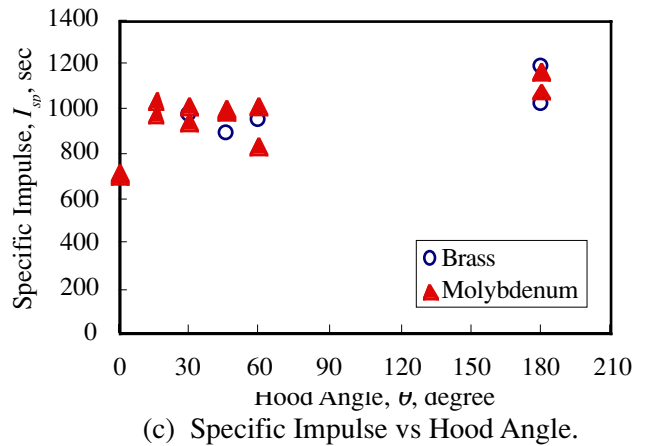
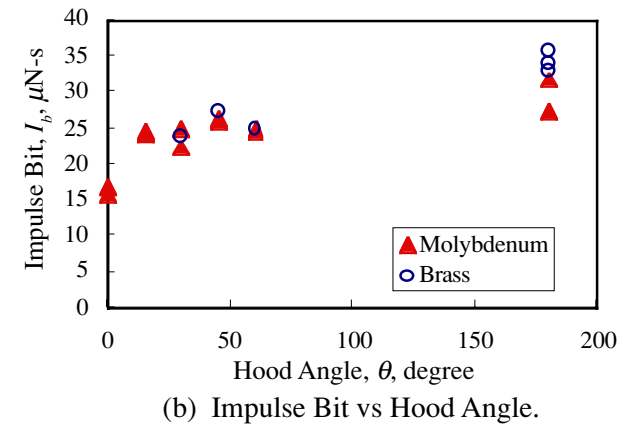
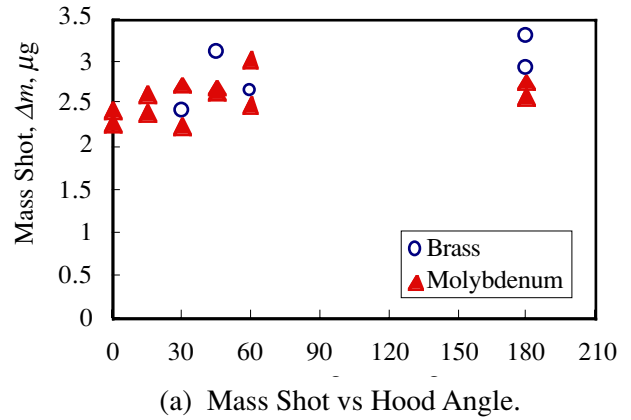
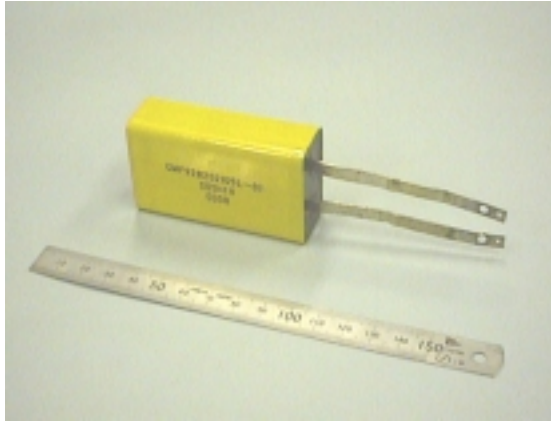


Fig. 8 The Performance of PPT with Hood.



(a) 1.0 μF Block-Type Capacitor



(b) 1.5 μF Plate-Type Capacitor (EM Capacitor)

Fig. 9 The Capacitors of BBM and EM.

Table 3 Specification of BBM and EM Capacitor.

(a) Specification of 1.0 μF Block-Type Capacitor.

No.	Max Voltage	Insulation resistance, $\text{M}\Omega$	Capacitance, μF	Dielectric Loss Tangent, %	Mass, g	Inductance, nH
1	4.0 kV DC	5X103	1.057	0.24	141	15.4
2	4.0 kV DC	5X103	1.059	0.24	140	15.4
3	4.0 kV DC	5X103	1.057	0.24	141	15.4

(b) Specification of 1.5 μF Plate-Type Capacitor.

No.	Max Voltage	Insulation resistance, $\text{M}\Omega$	Capacitance, μF	Dielectric Loss Tangent, %	Mass, g	Inductance, nH
14	4.0 kV DC	$> 3 \times 10^3$	1.470	0.36	186.0	41.1
15	4.0 kV DC	$> 3 \times 10^3$	1.472	0.37	184.8	44.0

about 40 degree, the impulse bit of the operation with 30 degree hood should decrease in our experiment. But, we can assume that the discharge phenomenon of PPT occur at not only propellant surface but also the discharge channel between the cathode and anode. With the consideration of this assumption, the 15 degree hood should substantially have more opening angle for charged particles, we can understand the reason 15 degree hood operation indicated almost the same impulse bit as 30, 45, 60 degree hood operation. So, the hood should be designed in order to prevent the neutral particles from spreading and not to effect the momentum of charged particles.

In the design of EM system, we adopt the 30 degree hood because the charring problem sometimes occurred with 15 degree hood in our experiment. But this reason of the charring was not obvious now.

Capacitor Development

As mentioned before, we operated PPT at about 2.3 J for ETS-IV, TMIT-12, TMIT-6a and TMIT-5 since the R & D of TMIT-PPT started. At this energy level operation, we used two 1.0 μF mica-paper capacitors in parallel for getting about 2.0 μF capacitance because of the discharge voltage to be fixed at about 1,500 V. However, at the evaluation of long time operation durability with TMIT-5, non uniform ablation and charring problem occurred. Therefore we changed the capacitance from 2.0 μF to 3.0 μF (1.0 $\mu\text{F} \times 3$) and increased discharge energy from 2.4 J to 3.6 J on maintaining the discharge voltage to be 1,500 V.

TMIT-PPT will be composed of independent three component and be designed to have flexibility of the relative position of these components. Particularly for μ -LabSat II, however, HEAD unit will be designed to be put on the CAP BANK. In this case, the system assembly height will not be small if we adopt the block-type capacitor for CAP BANK EM.

So, we adopt the plate-type 1.5 μF capacitor ($\times 2$) for EM system. Figure 9 and Table 3 show the appearance and specification of 1.0 μF block-type capacitor and 1.5 μF plate-type capacitor. The reason of the inductance increase of 1.5 μF plate-type capacitor seemed to be caused by its plate-like shape.

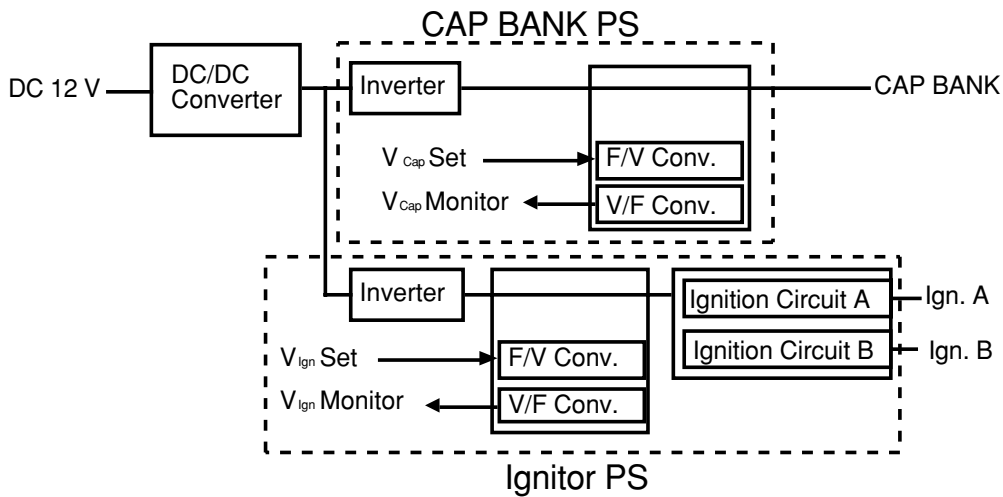


Fig. 10 Schematic Block Diagram of PPU

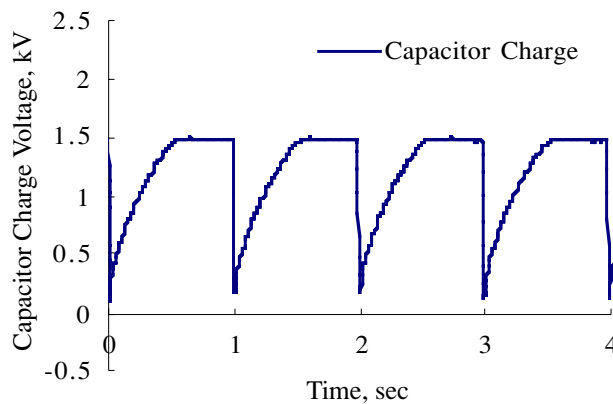


Fig. 11 Profiles of Capacitor Charge Voltage (3.3 J, 1 Hz operation)

PPU Development

In TMIT-PPT design, one PPU includes two power supplies (capacitor charge power supply and ignition power supply), and ignition power supply has the two output for Thruster Head A or B. Up to now, telemetry / command interface between μ -LabSat II satellite system and the bus voltage are not fixed, the installed interface is tentative. Therefore we temporarily have operated TMIT-PPT system at DC 12 V bus voltage. Figure 10 shows the schematic block diagram of PPU. And Fig. 11 shows the waveforms of the capacitor charge voltage for 3.3 J (1.5 kV charge to 2.95 μ F capacitor) discharge energy at 1 Hz.

Thruster - Capacitor Line

Considering the feasibility of the thruster system assembly, TMIT-PPT is categorized to three components and is designed to permit the layout of each component to be flexible. But, the relative distance between the thruster heads and the capacitor bank affects the PPT performance because the change of harness length between the thruster heads and the capacitor bank changes the circuit parameters of discharge and results in the change of PPT performance. Then, we evaluated PPT performance with TMIT-5 type thruster head with molybdenum electrodes using the following three types of harness.

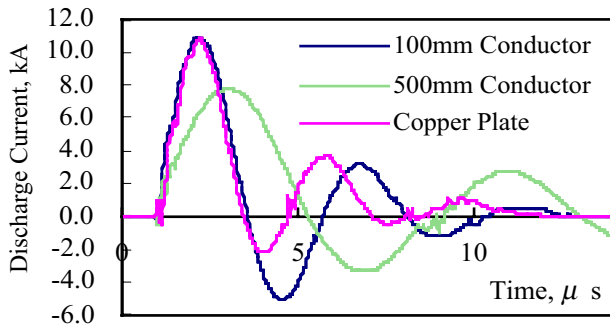


Fig. 12 Discharge Current Waveform

1. Copper plate : $S = 7 \text{ mm}^2$, $L = 70 \text{ mm}$
2. 100mm Conductor : $S = 0.75 \text{ mm}^2$, $L = 100 \text{ mm}$
3. 500mm Conductor : $S = 0.75 \text{ mm}^2$, $L = 500 \text{ mm}$

Table 4 Performance of PPT by Different in Connect Way between CAP BANK and Thruster Head

	500mm	100mm	Copper Plate
Impulse Bit, $\mu \text{ N-s}$	21.0	33.1	30.3
Mass Shot, $\mu \text{ g/sho}$	2.47	3.56	3.16
Specific Impulse, s	867	949	978
Peak current, kA	7.80	11.20	10.82
Period, $\mu \text{ s}$	7.76	4.58	3.56
Inductance, nH	467	161	106
Resistance, $\text{m}\Omega$	117	79	58
Capacitance, $\mu \text{ F}$	3.19	3.19	3.19

The experimental results are shown in Fig. 12 and Table 4. Figure 12 shows the discharge current waveforms measured with Rogowski coil. And Table 4 shows the change of the PPT performance and the discharge circuit parameters calculated from the current waveforms. As shown in this table, the mass shot and impulse bit decreased with increasing the resistance and inductance predictably. But, specific impulse did not decrease to the extent that the mass shot and impulse bit did. Assuming the PPT is equipped with a small satellite 500 mm, harnesses seem to have enough length, therefore, the performance of TMIT-PPT seemed to be not affected greatly using up to 500mm harnesses.

Present Status

At present, we have evaluated the performance of EM system. Figure 13 shows the appearance of TMIT-PPT EM assembly. As mentioned before, TMIT-PPT is consist of three components (two thruster heads, one PPU and one capacitor bank). And in EM phase, there are two types of thruster head. One is the “HEAD-EM

Table 5 TMIT-PPT EM-01 Mass Breakdown

Component	Part	Mass, g
HEAD	HEAD-EM01str. (dry mass)	115
	HEAD-EM01can. (dry mass)	107
CAP BANK	Capacitor ($1.5\mu\text{F} \times 2$)	371
	Housing	185
PPU	Electronics	200
	Housing	135
Others	HEAD, Plate, Cable, Screw, etc	135
Total		1367

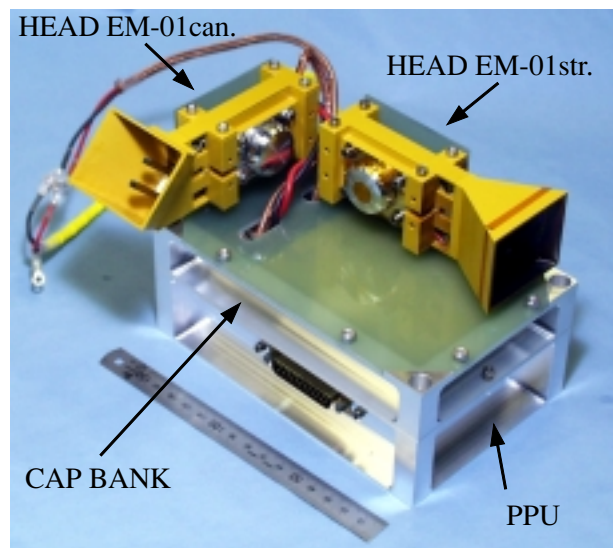


Fig. 13 TMIT-PPT EM-01 Assembly

Table 6 Scheduled and Achieved Performance (in EM phase)

Items	Target	Achieved (EM)
Satellite Mass	< 50 kg	
Capacitor		2.95 μ F
Charge Voltage	1,500 V (Nominal) 1,000 ~ 2,000 V	1,500 V (Nominal) 1,200, 1,500, 1,800 V
Charge Energy		3.3 J 2.1, 3.3, 4.8 J
Pulse Rate		0.75 Hz (Nominal) 0.5, 0.75, 1.0 Hz
Electrical Power	4 W (Nominal)	4.2 W (Nominal)
Impulse Bit		21.45 μ Ns
Mass Shot		2.27 μ g
Specific Impulse	> 800 s	960 s
Total Impulse	60 N-s	8.25 N-s [#]
Dry Weight	Total < 2.0kg	1.367 kg*
Size	< 210 × 148 mm	173 × 110 mm

*Excluding MLI etc.

#Obtained in H-MST in BBM phase

str.” whose thrust axis corresponds with the propellant feed axis, and the other is the “HEAD-EM can.” whose thruster axis is canted against the propellant feed axis in the perpendicular plane of electrodes. In the design for μ -LabSat II, “HEAD str.” and “HEAD can.” which has 45 degree cant angle will be on board.

Tables 5 and 6 show the mass breakdown and the scheduled and achieved performance of TMIT-PPT in EM phase. The total mass and specific impulse are currently about 1.4 kg and 960 s, we can achieved the target (< 2.0 kg and > 800 sec).

For future works, we will evaluate the durability of long time operation and will conduct the environmental test (thermal vacuum, vibration etc. at QT level) in EM phase.

Conclusion

In this paper, the design consideration and present status of TMIT-PPT are described. In the design of Thruster Head, the change of sublimation area, energy density, electrode material, and hood angle were described. The results of these evaluation are approximately as follows.

By miniaturizing sublimation area (from 5 cm² to 0.5 cm²) and increasing energy density (from 0.5 J/cm² to 7.2 J/cm²), the charring and no uniform sublimation problem were solved, and about 960 sec of specific impulse was achieved.

For the design of EM system, we decided the hood angle (30 degree), capacitance of main discharge capacitor (1.5 μ F × 2, 2.95 μ F), discharge energy (3.3 J / shot) and so on. In EM phase, the system mass and is about 1.4 kg.

Acknowledgments

The authors would like to express their sincere thanks to Dr. Kyo Kuriki ,a commissionair of Minister of Education, Culture, Sports, Science and technology, commissioner, Prof. Toki of ISAS, Prof. Arakawa of Tokyo University, and Prof. Tachibana of Kyushu Institute of Technology for their useful suggestions.

The authors would like to acknowledge Ms. Miwa Igarashi (presently Mitsubishi Electric Engineering Co.

Ltd.) who had developed the TMIT-PPT together with us in TMIT.

This work is supported in part by the Grant-in-Aid for Science Research (A) of Japan Society for the Promotion of Science.

References

1. Hirata, M., *et al*, "Electromagnetic Noise Measurement Study of Pulsed Plasma Engine," AIAA-81-0722
2. Hirata, M. and Murakami, H., "Development of a Pulsed Plasma Engine," *17th International Electric Propulsion Conference*, Tokyo, Japan, IEPC-84-48, 1984.
3. Noda, A., *et al*, "Concept Design of μ -Lab Sat II," *44th Space Sciences and Technology Conference*, Fukuoka, Japan, 00-3E13, 2000. (in Japanese)
4. Burton, R. L. and Turchi, P. J., "Pulsed Plasma Thruster," *Journal of Propulsion and Power* **14**, No. 5, 716-735 September-October, 1998.
5. Rayburn, C., Campbell, M., "Development of a Micro Pulsed Plasma Thruster for the Dawgstar Nanosatellite," *36th Joint Propulsion Conference*, Huntsville, Alabama, AIAA 2000-3256, 2000.
6. Hoskins, W. A. *et al.*, "PPT Development Efforts at Primex Aerospace Company," *35th Joint Propulsion Conference*, Los Angeles, USA, AIAA-99-2291, 1999.
7. Benson, S. W., Arrington, L. A., Hoskins, W. A. and Meckel, N. J. "Development of a PPT for the EO-1 Spacecraft," *35th Joint Propulsion Conference*, Los Angeles, USA, AIAA-99-2276, 1999.
8. Hirata M., Murakami H., "Exhaust Gas Analysis of a Pulsed Plasma Engine," *17th International Electric Propulsion Conference*, Tokyo, Japan, IEPC-84-52, May, 1984
9. Myers, R.M., Arrington, L.A., Pencil, E., Carter, J., Heminger, J., Gatsonis, N., "Pulsed Plasma Thruster Contamination," *32nd Joint Propulsion Conference*, Lake Buena Vista, FL, AIAA-96-2729, July 1-3, 1996.
10. Guman, W. J. and Begun, M., "Exhaust Plume Studies of a Pulsed Plasma Thruster," *13th International Electric Propulsion Conference*, San Diego, USA, AIAA-78-704, April 25-27, 1978
11. Vondora, R., Thomassen, K., and Solbes, A., "A Pulsed Electric Thruster for Satellite Control." *Proceedings of the IEEE* **59**, No. 2, 271-277, February, 1971.